Ph

JOURNAL DE PHYSIQUE

Tome 49 | Colloque C8, supplément au n° 12 | décembre 1988

Proceedings of the International Conference on Magnetism

Part II

Paris, France
July 25-29, 1988

Editor : D. Givord

les éditions de physique

Avenue du Hoggar,
Zone Industrielle de Courtabœuf,
B.P. 112,
F-91944 Les Ulis Cedex, France

CONTENTS

PART I

Chapter 2. Weak ferromagnetism, invar anomaly, magnetic transitions in itinerant systems

Chapter 3. Rare-earth and actinides: metals, alloys and compounds

Chapter 5. Intermediate valence, Kondo and heavy fermions

PART II

Chapter 6. Magnetic properties of non-metallic systems

Chapter 7. Spin-glasses

Chapter 8. Magnetism and disorder

Chapter 9. Amorphous magnets

Chapter 10. Low-dimensional systems

Chapter 11. Critical phenomena, magnetic excitations and chaos

PART III

Chapter 12. Surface magnetism, ultra-thin films, superlattices

Chapter 13. Thin films, multilayers, small particles

Chapter 14. Domains, walls, hysteresis phenomena

Chapter 15. Magnetic recording, other applications and cross-disciplinary

JOURNAL DE PHYSIQUE
Colloque C8, Supplément au n° 12, Tome 49, décembre 1988

CRITICAL DYNAMICS OF FERROMAGNETS

E. Frey and F. Schwabl

Institut für Theoretische Physik, Physik-Department der Technischen Universität München, James Franck Straße, D-8046 Garching, F.R.G.

Abstract. – The crossover in the dynamics from isotropic to dipolar critical behaviour has been a matter of debate over many years. We review a mode coupling theory for dipolar ferromagnets which gives a unified explanation of the seemingly contradictory experimental situation. The shape functions, the scaling functions for the damping coefficients and the precise position of the crossover are computed. Below T_c only the exchange interaction is taken into account.

1. Introduction.

Ferromagnets in the vicinity of their Curie point were among the first systems where critical dynamical phenomena with non classical features were observed experimentally. Theoretically a qualitative and increasingly quantitative understanding was provided by dynamical scaling theory, mode coupling (MC) theory and the renormalization group (RG) theory. In the region where the exchange interaction dominates, the MC theory was particularly successful for isotropic Heisenberg ferromagnets [1].

A qualitative understanding can be obtained by combining dynamical scaling with hydrodynamics. According to hydrodynamics, in the ferromagnetic phase the spin wave resonance is given by $\pm q^2\mathcal{D} - iq^4\Lambda$ as a function of the wave number q. The stiffness constant $\mathcal{D}$ is related to the transverse static susceptibility χ_q^{T}, the magnetization M and the correlation length ξ by $q^2\mathcal{D} = \frac{M}{\chi_q^{\mathrm{T}}} \propto q^2\xi^{-\frac{1}{2}(1-\eta)}$. If this is combined with the dynamical scaling hypothesis for the critical frequency,

$$\omega_c = q^z\Omega\left(q\xi\right), \tag{1.1}$$

one finds

$$z = \frac{5-\eta}{2}. \tag{1.2}$$

Using again (1.1) and (1.2) the damping coefficient Λ of the spin waves and the spin diffusion coefficient D of the paramagnetic phase are $\Lambda \sim \xi^{\frac{3+\eta}{2}}$ and $D \sim \xi^{-\frac{1}{2}(1-\eta)}$.

Because of the long range character of the dipole-dipole interaction it dominates the critical behaviour in the immediate vicinity of the critical point and for small wave vectors. If the dipolar interaction is weak compared to the exchange interaction, there is a crossover from isotropic critical behaviour to dipolar critical behaviour [2]. The static crossover can be characterised by a wave vector q_{D}. It turns out that the static critical exponents of the dipolar fixed point are very close to the isotropic [2]. The most significant crossover can be seen in the longitudinal susceptibility, which is equal to the transverse susceptibility for ξ^{-1} and $q \gg q_{\mathrm{D}}$ and remains finite in the opposite limit. Hence one expects a crossover to purely relaxation dynamics with a critical exponent $z = 2 + c\eta$. A widely held belief is that this crossover should take place at q_{D}. Indeed this crossover was found in the local relaxation time in hyperfine intraction (HFI) experiments and the presence of dipolar forces manifests itself also in electron spin resonance (ESR) experiments. On the other hand in neutron scattering experiments the dynamic crossover could not be detected. Right at T_c the critical behaviour was found to be isotropic down to almost a tenth of q_{D}. What made the situation even more bewildering was the fact that nevertheless neutron scattering data could not be fitted by the Resibois-Piette scaling function. Another important problem is the shape function, which was found to decay nearly exponentially by spin echo experiments on EuO. Non of the theories, MC as well as RG, based on the short range exchange interaction could explain this feature.

We review a recent MC theory for dipolar ferromagnets [3, 4] on the basis of which these bewildering and seemingly conflicting features can be explained in a unified fashion.

2. Dipolar ferromagnets.

2.1 Mode coupling equations for dipolar ferromagnets. – The Hamiltonian for a spin system with both short range exchange and long range dipolar interactions is given by [2]

$$H = \int \frac{\mathrm{d}^3q}{(2\,\pi)^3}\left[\left(J_0 + Jq^2\right)\delta^{ij} + \right.$$
$$\left. + Jg\,\frac{q^iq^j}{q^2}\right] S^i\left(\mathbf{q}\right)S^j\left(-\mathbf{q}\right). \tag{2.1}$$

The parameter g characterises the ratio of dipolar to exchange interaction J. Due to the symmetry of the

Hamiltonian it is necessary to decompose the spin operator $\mathbf{S}(\mathbf{q})$ into a longitudinal and two transverse components with respect to the wave vector $\mathbf{S}(\mathbf{q}) = S^{\mathrm{L}}(\mathbf{q})\,\hat{\mathbf{q}} + S^{\mathrm{T}_1}(\mathbf{q})\,\hat{\mathbf{t}}^1(\hat{\mathbf{q}}) + S^{\mathrm{T}_2}(\mathbf{q})\,\hat{\mathbf{t}}^2(\hat{\mathbf{q}})$, where the orthonormal set of unit vectors is defined by $\hat{\mathbf{q}} = \mathbf{q}/q$, $\hat{\mathbf{t}}^1(\hat{\mathbf{q}}) = \mathbf{q}\times\mathbf{e}_3 \Big/ \left(q_1^2 + q_2^2\right)^{1/2}$ and $\hat{\mathbf{t}}^2(\hat{\mathbf{q}}) = \hat{\mathbf{q}}\times\hat{\mathbf{t}}^1(\hat{\mathbf{q}})$. For vanishing components of $\mathbf{q}$ the limits are taken in the order of increasing cartesian components. The Heisenberg equations of motion are of the general structure

$$\dot{S}^{\mathrm{L}}_{\mathbf{q}} = \cdots \left[\left(\mathbf{q}\,(2\,\mathbf{k} - \mathbf{q}) + \cdots g\right) \left\{ S^{\mathrm{T}_1}_{\mathbf{q}-\mathbf{k}},\ S^{\mathrm{L}}_{\mathbf{k}} \right\} + \cdots \right] \tag{2.2}$$

and for $S^{\mathrm{T}_1}_{\mathbf{q}}$ and $S^{\mathrm{T}_2}_{\mathbf{q}}$ correspondingly, where $\{\ ,\ \}$ denotes the anti-communator. The terms proportional to g, resulting from the dipolar term in the Hamiltonian remain finite as the wave vector q tends to zero, whereas all the other terms vanish in this limit. This reflects the fact that the dipolar forces lead to a relaxational dynamics in the limit of long wavelengths.

The quantities of interest are the longitudinal and transverse Kubo relaxation functions

$$\Phi^{\mathrm{L(T)}}(q,\ g,\ \omega) = \int_0^\infty \mathrm{d}t\ \mathrm{e}^{i\omega t}\Phi\left(S_q^{\mathrm{L(T_1)}},\ S_q^{\mathrm{L(T_1)}},\ t\right) = \\ = \frac{i}{\omega + i\Gamma^{\mathrm{L(T)}}(q,\ g,\ \omega)}, \tag{2.3}$$

where

$$\Phi(A,\ B,\ t) = i\lim_{\varepsilon\to 0}\int_t^\infty \mathrm{d}\tau\ \mathrm{e}^{-\varepsilon\tau}\left\langle\left[A(\tau),\ B(0)^+\right]\right\rangle$$

with the normalization $\Phi(A,\ B,\ t=0) = 1$.

Here $\Gamma^{\mathrm{L(T)}}(q,\ g,\ \omega)$ are the longitudinal and transverse damping functions. Because of the rotational symmetry around the wave vector $\mathbf{q}$ the correlation functions of $S_q^{\mathrm{T}_1}$ and $S_q^{\mathrm{T}_2}$ are equal.

Now we apply the standard procedure of MC theory [5]: (i) we write down the Kubo formula for the transport coefficients $\Gamma^{\mathrm{L(T)}}(q,\ g,\ \omega)$; (ii) we consider two mode decay processes, which amounts to a factorisation of the Kubo formulas [6]. This leads to two coupled integral equations ($\alpha \equiv \mathrm{T},\ \mathrm{L}$):

$$\Gamma^\alpha(q,\ g,\ t) = 2\,J^2 k_{\mathrm{B}}T\int\frac{\mathrm{d}^3k}{(2\,\pi)^3}\times\Bigg[v^\alpha_{\beta\sigma}(k,\ q,\ g,\ \eta)\left(\delta_{\sigma,\ \mathrm{T}} + \delta_{\alpha,\ \mathrm{T}}\delta_{\beta,\ \mathrm{L}}\delta_{\sigma,\ \mathrm{L}}\right)\times \\ \times\frac{\chi^\beta(k,\ g)\,\chi^\sigma\left(\left|\mathbf{q}-\mathbf{k}\right|,\ g\right)}{\chi^\alpha(q)}\Phi^\beta(k,\ g,\ t)\,\Phi^\sigma\left(\left|\mathbf{q}-\mathbf{k}\right|,\ g,\ t\right)\Bigg] \tag{2.4}$$

where $\eta = \cos\ (\mathbf{k},\ \mathbf{q})$. The vertex functions $v^\alpha_{\beta\sigma}$ for the decay of the mode α into the modes β and σ are proportional to $\hat{v}^\alpha_{\beta\sigma}$, the scaled vertex functions defined by $v^\alpha_{\beta\sigma}(k,\ q,\ g,\ \eta) = q^4\hat{v}^\alpha_{\beta\sigma}(y,\ \rho,\ \eta)$, which can be found in references [3, 4].

Now the essential point is that the MC equations (2.3) and (2.4) are consistent with the generalised dynamical scaling laws

$$\Gamma^a(q,g,\omega) = \Lambda q^z\Omega^\alpha(x,y)\,\gamma^\alpha(x,y,\nu_\alpha), \tag{2.5a}$$

$$\Phi^\alpha(q,g,\omega) = \frac{1}{\Lambda q^z\Omega^\alpha(x,y)}\varphi^\alpha(x,y,\nu_\alpha), \tag{2.5b}$$

where in the present case whe have to introduce the scaling variables

$$x = \frac{1}{q\xi},\quad y = \frac{\sqrt{g}}{q},\quad \text{and}\quad \nu_\alpha = \frac{\omega}{\Lambda q^z\Omega^\alpha(x,\ y)}. \tag{2.6}$$

The scaled frequencies contain the characteristic frequencies $\Omega^\alpha(x,\ y)$.

Inserting equation (2.5) together with the static scaling law $\chi^\alpha(q,\ g) = \frac{1}{Jq^2}\hat{\chi}^\alpha(x,\ y)$ into equations (2.3) and (2.4) one finds MC equations for the scaling functions [4].

The non universal frequency scale of equation (2.5) is found to be $\Lambda = a^{5/2}\sqrt{\frac{Jk_{\mathrm{B}}T}{4\pi^4}} = \frac{g_{\mathrm{L}}\mu_{\mathrm{B}}}{q_{\mathrm{D}}}\sqrt{\frac{k_{\mathrm{B}}Ta_1}{8\pi^4}}$.

The above relations contain the critical dynamic exponent $z = \frac{5}{2}$, where one has to realize that the crossover of the critical dynamic exponent is contained in the scaling functions for the transport coefficients $\gamma^\alpha(x,\ y,\ \tau_\alpha)$, the scaling functions for the Kubo relaxation functions $\varphi^\alpha(x,\ y,\ \tau_\alpha)$ and the characteristic frequencies $\Omega^\alpha(x,\ y)$.

If the transport coefficients vary only slowly with ω we may approximate our relaxation functions by Lorentzians; i.e. we replace the transport coefficients by their values at $\omega = 0$: $\Gamma^{\mathrm{L}}(q,\ g) = \Gamma^{\mathrm{L}}(q,\ g,\ \omega = 0)$ and $\Gamma^{\mathrm{T}}(q,\ g) = \Gamma^{\mathrm{T}}(q,\ g,\ \omega = 0)$. This additional approximation finally leads to a simplified set of coupled integral equations for the transverse and longitudinal linewidth above the transition temperature which obey the generalised dynamical scaling law

$$\Gamma^\alpha(q,\ g) = \Lambda q^z\gamma^\alpha(x,\ y). \tag{2.7}$$

The MC equations for the scaling functions are given by

$$\gamma^\alpha(x,y) = \frac{2\pi^2}{\hat{\chi}^\alpha(x,y)}\int_{-1}^1\mathrm{d}\eta\int_0^\infty\mathrm{d}\rho\sum_\beta\sum_\sigma\hat{v}^\alpha_{\beta\sigma}(y,\rho,\eta)$$

$$\times \left(\delta_{\sigma,\,\mathrm{T}} + \delta_{\alpha,\,\mathrm{T}}\delta_{\beta,\,\mathrm{L}}\delta_{\sigma,\,\mathrm{L}}\right) \times \frac{\rho_-^{-2}\hat{\chi}^{\beta}\left(\frac{x}{\rho},\frac{y}{\rho}\right)\hat{\chi}^{\sigma}\left(\frac{x}{\rho_-},\frac{y}{\rho_-}\right)}{\rho^{5/2}\gamma^{\beta}\left(\frac{x}{\rho},\frac{y}{\rho}\right)+\rho_-^{5/2}\gamma^{\sigma}\left(\frac{x}{\rho_-},\frac{y}{\rho_-}\right)} \qquad (2.8)$$

where $\rho = k\,/\,q$ and $\rho_- = |\mathbf{q}-\mathbf{k}|\,/\,q$. Concerning the critical dynamical exponent one finds for the longitudinal linewidth a crossover from $z = 2.5$ in the isotropic critical region to $z = 0$ in the dipolar critical region, whereas for the transverse linewidth the crossover is from $z = 2.5$ to $z = 2$. The precise position of this crossover can only be determined numerically.

As for the pure isotropic ferromagnet, the MC equations do not account for effects of the critical exponent η, which will be neglected in the following. In the numerical calculations we will use the Ornstein Zernike forms for the static susceptibilities $\chi^{\alpha}(q,g) = J^{-1}\left(q^2+\xi^{-2}+\delta_{\alpha,\mathrm{L}}\,g\right)^{-1}$, where $\xi = \xi_0\left((T-T_c)\,/\,T_c\right)^{-\nu}$ is the correlation length. The static crossover is contained in ξ through the effective exponent $\nu = \gamma_{\mathrm{eff}}\,/\,2$ [7].

2.1 Predictions of the theory

2.2.1 *Neutron scattering.* – In neutron scattering experiments one measures the cross-section for inelastic magnetic scattering. Therefore one is able to mesure the dynamical scaling functions as functions of both temperature and wave vector.

In experimental studies it is convenient to plot the linewidth as a function of the single scaling variable $x = 1\,/\,q\xi$. In figure 1 we display the transverse scaling function *versus* $x = 1\,/\,q\xi$ for different values of $\theta = \mathrm{arctg}\; g^{1/2}\,\xi = N\pi/40$ with $N = 0,\ 1,\ \ldots,\ 19$. The curve $N = 1$ is indistinguishable from the Resibois-Piette function, $N = 0$. If g is finite, the curves approach the Resibois-Piette function for small x and deviate therefrom with increasing x. For a given material, g is fixed and the parameterisation by θ corresponds to a parameterisation by $(T-T_c)$. The experimental results of Mezei on iron (Fig. 3 of Ref. [8] and Fig. 4 of Ref. [9]) taken at different temperatures show the $(q\xi)^{-1}$ dependence exhibited by the transverse scaling function (Fig. 1). In a quantitative comparison of the experiments with the theory it would be necessary (i) to reanalyse the data taking into account the crossover of the critical exponent γ (ii) to use the exact shape function in the determination of the line width (iii) and to consider theoretically additional relaxation mechanisms (uniaxial terms, spin orbit interaction leading to pseudo-dipolar forces, etc.), which are irrelevant asymptotically but may add to the line width in the non asymptotic region.

To examine the dipolar crossover precisely at the Curie point, figure 2 displays the scaling functions for the transverse and longitudinal width for $T = T_c$

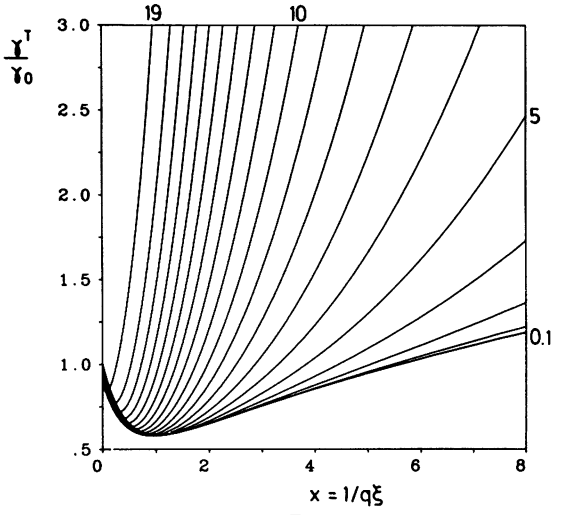

Fig. 1. – Scaling function γ^{T} for the transverse width *versus* $(q\xi)^{-1}$ for values of $\theta = N\pi\,/\,40$ with N indicated in the graph.

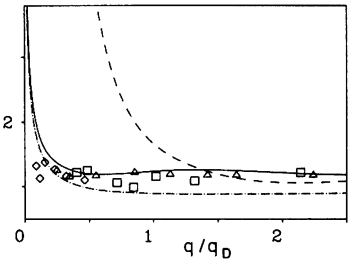

Fig. 2. – Scaling functions *versus* $y^{-1} = q\,/\,q_{\mathrm{D}}$ at T_c (in units of the theoretical non universal constant Λ) for (i) the half width at half maximum of the complete solution of the MC equations for the transverse Kubo function (solid), (ii) transverse (point-dashed) and (iii) longitudinal (dashed) linewidth in Lorentzian approximation. Experimental data for EuO ((□) Ref. [11]; (◇) Ref. [9]) and Fe ((△) Ref. [8]).

against the wave number; i.e. $y^{-1} = q\,/\,g^{1/2}$. These results clearly show that the crossover from isotropic to dipolar critical dynamics in the transverse linewidth occurs at a wave number smaller than q_{D}, the position of the static crossover, by almost an order of magnitude. This purely dynamical shift of the crossover explains why, within the accessible wave vector region, this crossover escaped the detection by neutron scattering experiments. There is, however, an indication of an increase in the data for the transverse width at the smallest momentum transfer [10], as predicted by the theory.

The crossover of the longitudinal width, from $z = 2.5$ to $z = 0$, is more pronounced and occurs in the immediate vicinity of q_{D}. It should be possible to test this prediction experimentally. The reason for the dif-

ferent location of the dynamic crossover is mainly due to the fact, that it is primarely the longitudinal static susceptibility which shows a crossover due to the dipolar interactions. Since the change in the static critical exponent is numerically small, the transverse static susceptibility is nearly the same as for ferromagnets without dipolar interaction. Hence the crossover in the transverse width is purely a dynamical crossover, whereas the crossover of the longitudinal width beeing proportional to the inverse longitudinal susceptibility is enhanced by the static crossover.

2.2.2 *Electron spin resonance and hyperfine interaction experiments.* – There are two more groups of experiments, which probe different aspects of the critical dynamics. In ESR experiments one measures the electron response function at zero wave vector and determines therefrom the Onsager coefficient. In HFI experiments one observes the nuclear relaxation rate due to the surrounding fluctuating electronic moments. Because the latter are local experiments the relaxation rate contains an integral over the wave vector space. From our theory we find [3, 12] that in these cases the dynamical crossover is essentially determined by the static quantities. Up to minor uncertainties in the static crossover the theory is in excellent quantitative agreement with experiment [13-15] without using any adjustable parameter for the temperature variable. The crossover in these experiments is located at $q_D.\xi = 1$.

2.2.3 *Shape function.* – Now we return to the complete MC equation (2.4) to determine the shape functions. These were solved recently at the critical temperature [4]. The result for the relaxation function at the wave vector $q = 0.024$ Å^{-1} is shown in figure 3 as the solid line *versus* time in nsec, where the theoretical value for the non universal scale $\Lambda = 7.1/5.1326$ meV Å$^{5/2}$ of EuO is used. There is excellent agreement with the experimental data of Mezei [16] for $t \leq 1$ nsec. The experimental data are above the theoretical curve for $t \geq 1$ nsec. This may be due to finite collimation effects in this time domain, as noted by Mezei [16]. To substantiate this point we have also plotted in figure 3 the relaxation function at $q = 0.028$ Å^{-1} (poind-dashed curve), which is significantly higher than the curve for $q = 0.024$ Å^{-1} for $t \geq 1$ nsec. The fairly large difference of the curves with $q = 0.024$ Å^{-1} and $q = 0.028$ Å^{-1} comes from the vicinity of the crossover region.

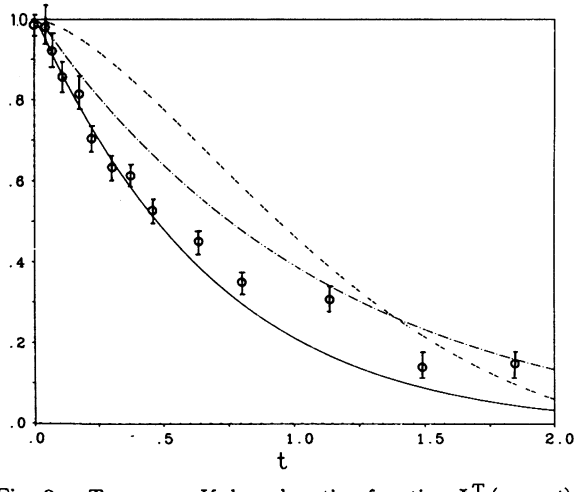

Fig. 3. – Transverse Kubo relaxation function $\Phi^T(q, g, t)$ at $q = 0.024$ Å^{-1} (solid line) and $q = 0.028$ Å^{-1} (point-dashed line) for dipolar ferromagnets *versus* time t in nsec. The dashed line is the transverse Kubo relaxation function for short range exchange interaction only at $q = 0.024$ Å^{-1}. Data points from figure 1 of reference [16].

In order to exhibit the difference from the MC theory including only short range exchange interaction, we have solved equations (2.3) and (2.4) for this special case; i.e. $y = 0$, $x = 0$ and $\rho_{\text{cut}} = \frac{q_{\text{BZ}}}{q}$ with $q = 0.024$ Å^{-1}. The result is the dashed curve in figure 3, which differs drastically from the lineshape including the long range dipolar interaction. Thus we conclude that the dipolar interaction is essential for the lineshape in the critical region. It is important to realize, that the crossover in the lineshape starts nearly at q_D, whereas the linewidth still scales with the isotropic critical dynamic exponen $z = \frac{5}{2}$ in this wave vector region.

In figure 2 the transverse linewidth at T_c obtained in the Lorentzian approximation is compared with the half width at half maximum (HWHM) resulting from the complete solution of the MC equations. Whereas these two functions are quite similar in shape, their asymptotic values differ by a factor of 1.2. The experimental data in figure 2 are divided by the theoretical value of the non universal constants. Thus there is agreement between experiment and the HWHM of the complete MC solution without adjustable parameters.

By comparing the MC results with RG calculations [17, 18], which neglect dipolar forces, one finds agreement in the wave vector and temperature region, where the influence of the dipolar forces is supposed to be weak.

Recently the complete MC equations were solved above T_c for EuS [19]. In figure 4 the transverse relaxation function at $T = 1.21\ T_c$ is shown *versus* the scaling variables $r = \left(x^2 + y^2\right)^{1/2}$ and τ_T. The crossover from a Gaussian like shape to a Lorentzian shape starts near the dipolar wave vector q_D similar as at $T = T_c$.

3. Isotropic ferromagnets below the Curie point

Below the Curie temperature the inclusion of dipolar forces is complicated because of two anisotropies (I) with respect to the direction of magnetisation and

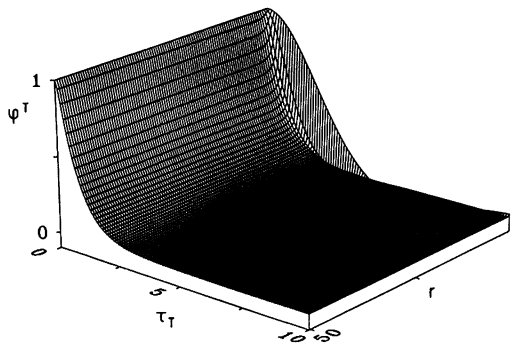

Fig. 4. – Scaling function for the transverse Kubo relaxation function $\varphi^{\mathrm{T}}(x, y, \tau)$ at $T = 1.21\ T_c$ for EuS *versus* $r = \left(x^2 + y^2\right)^{1/2}$ and τ_{T}.

(II) with respect to the wave vector. Therefore we limit ourselves to short range isotropic exchange interactions. Then the resulting scaling functions can be viewed as the analogues of the Resibois Piette [1] scaling function of the paramagnetic phase. The longitudinal and transverse linewidth $\Gamma(q)$ and $\Lambda(q)$ can be obtained within MC theory [3, 6].

Experimental investigations of the critical dynamics below T_c have been performed by means of unpolarized neutron scattering [20, 21]. However, only the side-peaks originating from the transverse spin waves have been detected, without any evidence for the central peak due to the longitudinal spin diffusion. This is plausible in the light of the MC results. In the hydrodynamical region ($x = 1 / q\xi \gg 1$) the width of the longitudinal peak is much wider than the separation of the transverse peaks [6]. Moreover, its intensity is smaller than that of the transverse magnons, which alltogether implies that it may be very difficult to distinguish the longitudinal peak from the background. In the critical region the linewidths are of the same order of magnitude. In this limit however the frequency of the transverse modes tends to zero. A first observation of the longitudinal peak was reported recently by Mitchell *et al.* [22] using polarized neutrons. However, there are not enough data to compare with the theoretical predictions, also, the material is disordered (palladium with 10 % iron).

In figure 5 we show $S^{xx}(q, \omega) = S^{yy}(q, \omega)$ and $S^{zz}(q, \omega)$ for parameters corresponding to EuO for a series of temperatures close to the Curie point where the wave vector is fixed to $q = 0.2$ Å^{-1}. In the presence of domains, such that the magnetization points with equal propability along the x, y and z-directions, one measures in neutron scattering experiments $S_{\mathrm{av}}(q, \omega) = (2S^{xx}(q, \omega) + S^{zz}(q, \omega)) / 3$, which is also shown in figure 5.

The qualitative similarity of $S_{\mathrm{av}}(q, \omega)$ to figure 4 of reference [21] is striking. For a quantitative comparison the theory has to be convoluted with the instrumental resolution function. In addition $S_{\mathrm{av}}(q, \omega)$ has to be multiplied by the detailed balance factor $\dfrac{\beta\omega}{1 - \mathrm{e}^{-\beta\omega}}$. And most important, close to T_c dipolar effects not contained in our theory for the ordered phase will be significant.

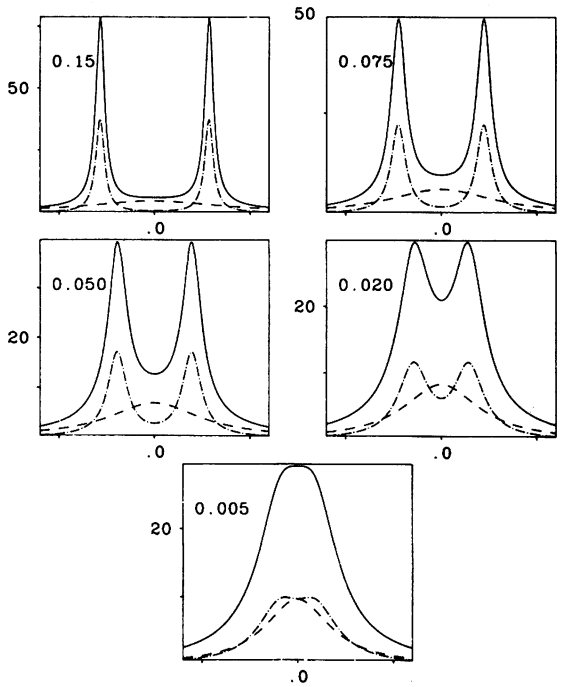

Fig. 5. – Dynamic structure functions $S^{xx}(q, \omega) = S^{yy}(q, \omega)$ (point-dashed), $S^{zz}(q, \omega)$ (dashed) and $3 \times S_{\mathrm{av}}(q, \omega)$ (solid) for EuO at the wave vector $q = 0.2$ Å^{-1}. The reduced temperatures are: a) 0.150, b) 0.075, c) 0.050, d) 0.020, e) 0.005.

Acknowledgments

This work has been supported by the German Federal Minister for Research and Technology (BMFT) under contract number 03-SC1TUM-0.

[1] Resibois, P. and Piette, C., *Phys. Rev. Lett.* **24** (1970) 514.

[2] Aharony, A. and Fisher, M. E., *Phys. Rev. B* **8** (1973) 3323.

[3] Frey, E. and Schwabl, F., *Phys. Lett. A* **123** (1987) 49; *Z. Phys. B* **71** (1988) 355.

[4] Frey, E., Schwabl, F. and Thoma, S., *Phys. Lett. A* **129** (1988) 343.

[5] Kawasaki, K., *Progr. Theor. Phys.* **39** (1968) 285; *Ann. Phys.* **61** (1970) 1; Phase Transitions and Critical Phenomena, Vol. 5a, Eds. Domb and Green (Academic Press) 1976.

[6] Schwabl, F., *Z. Phys.* **246** (1971) 13.
[7] Bruce, A. D., Kosterlitz, J. M. and Nelson, D. R., *J. Phys. C* **9** (1976) 825.
[8] Mezei, F., *Phys. Rev. Lett.* **49** (1982) 1096.
[9] Mezei, F., *J. Magn. Magn. Mater.* **45** (1984) 67.
[10] Böni, P., Shirane, G., Bohn, H. G. and Zinn, W., *J. Appl. Phys.* **61** (1987) 8.
[11] Böni, P., Shirane, G., *Phys. Rev. B* **33** (1986) 3012.
[12] Frey, E. and Schwabl, F., Proc. of the Conf. Nuclear Methods in Magnetims (Munich 1988) to be publ. In *Hyperf. Interact.*
[13] Kötzler, J., Scheithe, W. and Blickhan, R., *Solid State Commun.* **26** (1978) 641;
Kötzler, J., Kamleiter, G. and Weber, G., *J. Phys. C* **9** (1976) L361;
Kötzler, J. and von Philipsborn, H., *Phys. Rev. Lett.* **40** (1978) 790;
Kötzler, J. and Scheithe, W., *J. Magn. Magn. Mater.* **9** (1978) 4.
[14] Dunlap, R. A. and Gottlieb, A. M., *Phys. Rev. B* **22** (1980) 3422.
[15] Hohenemser, C., Chow, L. and Suter, R. M., *Phys. Rev. B* **26** (1982) 5056.
[16] Mezei, F., *Physica* **136B** (1986) 417.
[17] Dohm, V., *Solid State Commun.* **20** (1976) 657.
[18] Bhattacharjee, J. K. and Ferrell, R. A., *Phys. Rev. B* **8** (1981) 3323.
[19] Frey, E., Schwabl, F. and Thoma, S., to be published.
[20] Collins, M. F., Minkiewicz, V. J., Nathans, R., Passell, L. and Shirane, G., *Phys. Rev.* **179** (1969) 417;
Collins, M. F., Minkiewicz, V. J., Nathans, R. and Shirane, G., *Phys. Rev.* **182** (1969) 624.
[21] Dietrich, O. W., Als-Nielsen, J. and Passell, L., *Phys. Rev. B* **14** (1976) 4923.
[22] Mitchell, P. W., Cowley, R. A. and Pynn, R., *J. Phys. C* **17** (1984) L875.